SIGNAL TRANSDUCTION

Diurnal metabolic control in cyanobacteria requires perception of second messenger signaling molecule c-di-AMP by the carbon control protein SbtB

Khaled A. Selim[1,2]*†, Michael Haffner[1]†, Markus Burkhardt[1], Oliver Mantovani[3], Niels Neumann[1], Reinhard Albrecht[2], Roland Seifert[4], Larissa Krüger[5], Jörg Stülke[5], Marcus D. Hartmann[2], Martin Hagemann[3], Karl Forchhammer[1]*

Because of their photosynthesis-dependent lifestyle, cyanobacteria evolved sophisticated regulatory mechanisms to adapt to oscillating day-night metabolic changes. How they coordinate the metabolic switch between autotrophic and glycogen-catabolic metabolism in light and darkness is poorly understood. Recently, c-di-AMP has been implicated in diurnal regulation, but its mode of action remains elusive. To unravel the signaling functions of c-di-AMP in cyanobacteria, we isolated c-di-AMP receptor proteins. Thereby, the carbon-sensor protein SbtB was identified as a major c-di-AMP receptor, which we confirmed biochemically and by x-ray crystallography. In search for the c-di-AMP signaling function of SbtB, we found that both SbtB and c-di-AMP cyclase–deficient mutants showed reduced diurnal growth and that c-di-AMP–bound SbtB interacts specifically with the glycogen-branching enzyme GlgB. Accordingly, both mutants displayed impaired glycogen synthesis during the day and impaired nighttime survival. Thus, the pivotal role of c-di-AMP in day-night acclimation can be attributed to SbtB-mediated regulation of glycogen metabolism.

INTRODUCTION

Aerobic life on Earth evolved about 2.7 to 3.2 billion years ago with the evolution of oxygenic photosynthesis by cyanobacteria. Because photosynthesis uses energy provided by sunlight, cyanobacteria have evolved intricate circadian timing machinery to fine-tune photosynthesis and other metabolic activity to successive day-night cycles of different length (*1*). The recent discovery of a true circadian clock in the nonphotosynthetic bacterium *Bacillus subtilis* suggests that circadian rhythms may be widespread among other prokaryotes as well (*2*). All eukaryotic organisms independently evolved a circadian clock to acclimate to different diurnal cycles. In humans, the disruption of circadian timing correlates with diverse health problems including cancer and cardiovascular diseases (*3*).

Photoautotrophic organisms are constantly exposed to alternating day-night light regimes, which requires a permanent metabolic switch between autotrophic CO_2 fixation via Calvin-Benson cycle during the day and heterotrophic-like carbon catabolism during the night. During the day, newly fixed CO_2 is used for anabolic reactions, producing the building blocks for cell growth, and, in addition, for building up organic carbon reserves such as glycogen in cyanobacteria or starch in plants. During the night, glycogen is metabolized mainly using the oxidative pentose-phosphate (OPP) pathway, to provide reduction equivalents for energy conserving respiration (*4*, *5*). The constant switch between autotrophic and heterotrophic metabolism is operated by a sophisticated network of regulatory processes, which we only begin to understand. It involves sensing of the redox, energy, carbon, and nitrogen status as well as a specific timing machinery, the circadian clock (*1*, *3*, *6*). Although it is clear that the diurnal rhythm affects central carbon metabolism, mainly of glycogen anabolism and catabolism (*3*, *7*, *8*), our understanding of the signaling cascades regulating central carbon and nitrogen metabolisms under diurnal growth is still very preliminary.

Recent investigations pointed toward additional regulatory circuits, whose connection to the circadian clock is unclear. For instance, these reports revealed a noncanonical role of the second messengers cyclic di-adenosine monophosphate [3′,5′-c-di–adenosine 5′-monophosphate; hereafter c-di-AMP] and of the alarmone guanosine penta- and tetraphosphate ppGpp(p) in the diurnal photosynthetic lifestyle of cyanobacteria (*9*–*11*). Since its discovery in 2008, the second messenger c-di-AMP came into focus of research, owing to its essentiality in many organisms (*12*–*14*). This cyclic nucleotide has been implicated in regulating several biological processes, mainly related to cell wall and osmotic homeostasis in Firmicutes and, to a lesser extent, in Actinobacteria. In these heterotrophic bacteria, the main c-di-AMP targets are ion and osmolyte transporters, including those of K^+, Na^+, and Mg^{2+} ions, glycine betaine, and amino acids (*12*–*14*). Binding of c-di-AMP has also been demonstrated for a protein of the PII superfamily, termed DarA in *B. subtilis* (*15*) or PstA in *Staphylococcus aureus* (*16*); however, the physiological role of those signaling proteins remains unclear. In cyanobacteria, c-di-AMP has been recently described to be required for nocturnal dormancy of *Synechococcus elongatus*, because mutants of the c-di-AMP cyclase were impaired in nighttime survival. However, the molecular mechanism underlying the function of c-di-AMP in nocturnal dormancy has remained unresolved (*11*). In addition, the analysis of *Synechocystis* sp. mutants in which

[1]Organismic Interactions Department, Interfaculty Institute for Microbiology and Infection Medicine, Cluster of Excellence 'Controlling Microbes to Fight Infections', Tübingen University, Auf der Morgenstelle 28, 72076 Tübingen, Germany. [2]Department of Protein Evolution, Max Planck Institute for Developmental Biology, Tübingen, Germany. [3]Plant Physiology Department, Institute of Biological Sciences, Rostock University, Rostock, Germany. [4]Institute of Pharmacology, Hannover Medical School, Hannover, Germany. [5]Department of General Microbiology, Göttingen Center for Molecular Biosciences (GZMB), Göttingen University, Göttingen, Germany.
*Corresponding author. Email: khaled.selim@uni-tuebingen.de (K.A.S.); karl.forchhammer@uni-tuebingen.de (K.F.)
†These authors shared co-first authorship.

the c-di-AMP concentration was elevated or reduced implied a role for c-di-AMP in acclimation to abiotic stress and osmotic homeostasis (*17*). These findings agreed with the prediction of c-di-AMP–dependent riboswitches upstream of genes involved in ion homeostasis and osmolyte transport (*18*). Furthermore, expression of the *sll0505* gene, encoding the *Synechocystis* di-adenylate cyclase, showed a strong correlation with the acclimation to long-term nitrogen starvation. Upon resuscitating the chlorotic *Synechocystis* cells from nitrogen starvation, *sll0505* belonged to the strongest early up-regulated genes, implying a role of c-di-AMP in the awakening from dormancy (*19*). Although several c-di-AMP receptor proteins were identified in heterotrophic bacteria (*12*, *14*), the c-di-AMP targets and its signaling role in cyanobacteria remain elusive.

Another second messenger nucleotide that returned into the focus of interest is cyclic AMP (3′,5′-cAMP; hereafter cAMP), as it was revealed as effector molecule for the PII-like signaling protein SbtB. We identified SbtB as a unique component of the cyanobacterial carbon-concentrating mechanism (CCM), required for efficient acclimation to varying inorganic carbon (C_i) regimes (*20*). HCO_3^-/CO_2 metabolism is also strictly regulated by the diurnal metabolic status of the cells, with active C_i accumulation during the autotrophic day mode and arrest of HCO_3^- transport during nocturnal dormancy (*21*). Recently, it has been shown that the diurnal switch of C_i transport activity is regulated via phytochromes involving SbtB (*21*). The *sbtB* gene is located in an operon with the gene for the sodium-dependent bicarbonate transporter SbtA. A similar genetic arrangement is frequently found in proteins of the PII family, which cluster with the transport proteins they regulate. Accordingly, SbtB was proven as a regulator of SbtA transport activity (*20*, *22*, *23*). Similar to canonical PII proteins (*24*, *25*), SbtB perceives energy signals by binding adenosine 5′-triphosphate (5′-ATP) or adenosine 5′-diphosphate (5′-ADP), but unlike canonical PII proteins, SbtB also senses 5′-AMP and preferentially binds the second messenger cAMP (*20*). The cAMP concentration was correlated with the CO_2 supply of the cells, implying an evolutionary conserved role of the second messenger cAMP as an indicator of the cellular carbon status via SbtB signaling (*20*, *26*). Furthermore, structural analysis of SbtB revealed a putative redox-sensitive motif at the C terminus (*20*), suggesting that SbtB may play a role in controlling HCO_3^- transport in response to light/dark-mediated redox stimuli.

The binding of a broad range of adenine nucleotides suggested that SbtB may also bind c-di-AMP. Because our preliminary data confirmed this assumption, we set out to verify the physiological relevance of c-di-AMP binding to SbtB in the cyanobacterial model organism *Synechocystis* sp. PCC 6803 (hereafter *Synechocystis*). The c-di-AMP pull-down experiment to fish in vivo c-di-AMP receptors notably retrieved SbtB as the most enriched protein. The SbtB-c-di-AMP complex could pull down another target of central carbon metabolism, the glycogen-branching enzyme GlgB. C-di-AMP signaling via SbtB turned out to be pivotal for the diurnal lifestyle of *Synechocystis* through regulation of glycogen metabolism via GlgB.

RESULTS

SbtB is the major c-di-AMP receptor protein in *Synechocystis*

The SbtB signaling proteins are highly conserved in cyanobacteria and act as C_i-sensing module using energy and carbon signal inputs through binding of the adenine nucleotides ATP, ADP, and AMP as well as cAMP (*20*, *23*, *27*). This unique ability of SbtB to bind a wide variety of adenine-based nucleotides made it likely that SbtB could also bind the second messenger c-di-AMP. Using isothermal titration calorimetry (ITC), we tested the ability of recombinant SbtB protein from *Synechocystis* (*Sc*SbtB) to bind c-di-AMP. The trimeric *Sc*SbtB was able to bind with high affinity to c-di-AMP (Fig. 1A) with dissociation constant (K_d) values (K_{d1} of 2.3 μM, K_{d2} of 12.2 μM, and K_{d3} of 35.9 μM for the first, second, and third binding site of trimeric *Sc*SbtB, respectively) comparable to that of cAMP but stronger than that of ATP, ADP, and AMP (*20*). Moreover, the binding enthalpy for c-di-AMP was almost equivalent or higher than that of ATP, ADP, and AMP at a lower concentration of c-di-AMP (fig. S1), which indicates preferential binding to c-di-AMP over standard adenine nucleotides. To test whether binding to c-di-AMP is a common trait among SbtB proteins in cyanobacteria, we examined the ability of the SbtB protein from the filamentous cyanobacterium *Nostoc* sp. PCC 7120 (*Ns*SbtB) to bind c-di-AMP. Similar to *Sc*SbtB protein, ITC analysis revealed that *Ns*SbtB is able to bind c-di-AMP as well.

To reveal whether c-di-AMP binding to SbtB proteins is of physiological relevance, we performed a pull-down experiment with a crude cell extract from *Synechocystis* using immobilized c-di-AMP as a bait and searched for protein preys that specifically bound to c-di-AMP (Fig. 1B). The *Sc*SbtB protein, encoded by *slr1513*, was the highest enriched protein in the pull-down fraction (Fig. 1B), confirming that *Sc*SbtB is a real target of c-di-AMP signaling. In addition to *Sc*SbtB, we identified several transporters, among them the major potassium transporters in *Synechocystis* KtrA (*sll0493*), TrkA (*slr0773*), and MthK (*sll0993*). Moreover, the magnesium transporter MgtE (*slr1216*), the sodium/H^+ antiporters NhaS2 and NhaS5 (*sll0273* and *slr0415*, respectively), and the glutamate-Na^+ symporter (*slr0625*) were identified as c-di-AMP–binding proteins. In addition to SbtB, the identification of these potential c-di-AMP–dependent transporters implied that c-di-AMP may play a major role in regulating ionic and osmotic homeostasis of *Synechocystis*. KtrA, TrkA, and MgtE are also well-known c-di-AMP target proteins in Gram-positive bacteria (*12*, *14*, *28*); their successful identification here validated our pull-down assay. None of the c-di-AMP target proteins was identified in the negative control experiment.

Collectively, these results established SbtB as yet another PII-like protein interacting with c-di-AMP. Because the function of c-di-AMP sensing by this protein family remains obscure, we focused our investigation on the detailed characterization of the SbtB:c-di-AMP molecular interaction and its physiological consequences.

Structural basis of c-di-AMP binding to SbtB

To gain deeper insight into the structural basis of c-di-AMP binding by *Sc*SbtB, we aimed to obtain the crystal structure of the *Sc*SbtB:c-di-AMP complex. To this end, we used crystals that we previously obtained in different ligandation states from several cocrystallization trials of *Sc*SbtB (*20*). These crystals contain one *Sc*SbtB trimer in the asymmetric unit in space group $P3_2$, such that the three monomers and the three ligand binding sites, which are situated between the subunits, are involved in different crystal contacts (*20*). We now used apo crystals of this form in soaking experiments with c-di-AMP, resulting in a 2.0 Å crystal structure of the *Sc*SbtB:c-di-AMP complex (Fig. 1, C to F). However, only two of the binding sites turned out to be occupied by c-di-AMP (Fig. 1C), both with clear electron density for c-di-AMP in full occupancy (Fig. 1D). In these two sites,

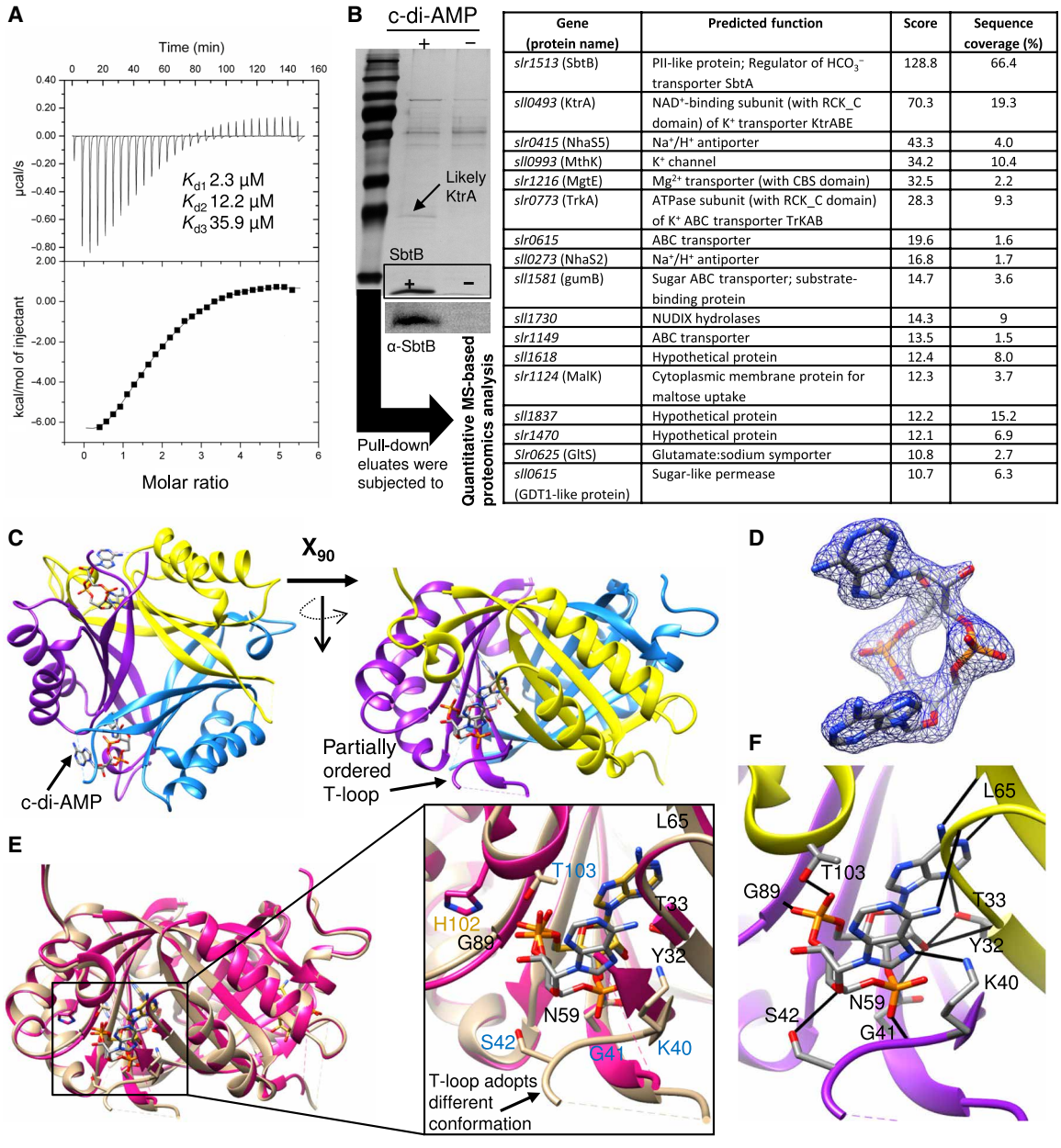

Gene (protein name)	Predicted function	Score	Sequence coverage (%)
slr1513 (SbtB)	PII-like protein; Regulator of HCO_3^- transporter SbtA	128.8	66.4
sll0493 (KtrA)	NAD^+-binding subunit (with RCK_C domain) of K^+ transporter KtrABE	70.3	19.3
slr0415 (NhaS5)	Na^+/H^+ antiporter	43.3	4.0
sll0993 (MthK)	K^+ channel	34.2	10.4
slr1216 (MgtE)	Mg^{2+} transporter (with CBS domain)	32.5	2.2
slr0773 (TrkA)	ATPase subunit (with RCK_C domain) of K^+ ABC transporter TrKAB	28.3	9.3
slr0615	ABC transporter	19.6	1.6
sll0273 (NhaS2)	Na^+/H^+ antiporter	16.8	1.7
sll1581 (gumB)	Sugar ABC transporter; substrate-binding protein	14.7	3.6
sll1730	NUDIX hydrolases	14.3	9
slr1149	ABC transporter	13.5	1.5
sll1618	Hypothetical protein	12.4	8.0
slr1124 (MalK)	Cytoplasmic membrane protein for maltose uptake	12.3	3.7
sll1837	Hypothetical protein	12.2	15.2
slr1470	Hypothetical protein	12.1	6.9
Slr0625 (GltS)	Glutamate:sodium symporter	10.8	2.7
sll0615 (GDT1-like protein)	Sugar-like permease	10.7	6.3

Fig. 1. Identification of SbtB as a major c-di-AMP receptor protein in cyanobacteria. (**A**) ITC analysis shows that SbtB binds c-di-AMP in an anticooperative manner with K_d values as indicated. Top: The raw ITC data in the form of the heat produced during the titration of 33.3 µM SbtB (trimeric concentration) with 0.5 mM c-di-AMP. Bottom: The binding isotherms and the best-fit curves according to the three sequential binding site model. (**B**) SDS–polyacrylamide gel electrophoresis analysis of c-di-AMP pull-down elution fraction and Western blot detection of SbtB, using α-SbtB antibodies. Samples were analyzed with quantitative MS-based proteomics analysis. Identified proteins are sorted by their scores. NAD^+, nicotinamide adenine dinucleotide; ATPase, adenosine triphosphatase; ABC, ATP-binding cassette; NUDIX hydrolases cleave nucleoside diphosphates linked to any ("x") moiety. (**C** to **F**) Structural and binding properties of the *Sc*SbtB protein. (C) Overall architecture of the trimeric SbtB:c-di-AMP complex with nucleotide-binding pockets located in the intersubunit clefts and shown in ribbon representation with different color for each monomer. (D) The electron density of c-di-AMP is shown as an F_o-F_c omit map contoured at 2.5 σ. (E) Superposition of *Sc*SbtB:c-di-AMP (brown) with *Sc*SbtB:AMP (pink; PDB: 5O3R), yielding an root mean square deviation of 0.33 Å and showing that the T-loop in the SbtB:c-di-AMP complex is partially ordered and adopts a different conformation than in the SbtB:AMP structure. (F) Close-up of the c-di-AMP binding site with relevant residues for nucleotide binding shown as sticks, and H bonds indicated by thin lines. (*E*) Inset: Highlighting the superposition of the nucleotide binding sites, with residues specific for c-di-AMP binding labeled in blue and those for AMP in orange.

as compared to the AMP- or cAMP-bound complexes, the base of the T-loop was found in a different conformation (Fig. 1E), forming additional interactions with the ligand (Fig. 1F), while the third site remained in apo-state due to limitations of the crystal packing. To exclude that also the folding of the T-loop or other binding-induced conformational changes were possibly restrained by crystal contacts during the soaking experiment, we also performed cocrystallization trials with c-di-AMP. Unexpectedly, these again yielded the same

crystal form resulting in a dataset of similar resolution, with the same two sites occupied and no noticeable structural differences.

All three subunits of the *Sc*SbtB:c-di-AMP complex are essentially in the same conformation as in the apo-*Sc*SbtB coordinates, and the whole *Sc*SbtB:c-di-AMP complex superimposes with a Cα–root mean square deviation value of 0.26 Å on the apo-*Sc*SbtB trimer [Protein Data Bank (PDB): 5O3P] (fig. S2). While there were no major differences between the *Sc*SbtB:c-di-AMP complex and apo-*Sc*SbtB, a comparison with the AMP- or cAMP-bound complexes revealed several additional unique interactions between c-di-AMP and the base of the T-loop (Fig. 1, E and F, and fig. S2), which caused a partial ordering and restructuring of the loop (Fig. 1, C to F). Structural alteration of the T-loop is a characteristic mechanism by which effector molecules modulate the interaction of canonical PII proteins with their receptors (*25*, *29*). The effect of c-di-AMP binding on the T-loop conformation strengthened the above results on the specificity of c-di-AMP binding to SbtB and suggested that c-di-AMP signaling via SbtB is functionally relevant and affects SbtB interaction with diverse interaction partners.

Physiological role of SbtB as a c-di-AMP receptor protein

Next, to search for a functional link between SbtB as a c-di-AMP receptor protein and c-di-AMP signaling cascade, we aimed to compare the phenotype of a *sbtB*-deficient mutant (encoded by *slr1513*) with a mutant deficient in *dacA*, which encodes for the only identified di-adenylate cyclase A (DacA; encoded by *sll0505*) in *Synechocystis*. To create a c-di-AMP free mutant, we first attempted the generation of a deletion or insertion Δ*dacA* mutant in a glucose-sensitive background (GS-strain). The insertion attempt aimed to avoid a polar effect on the expression of the downstream gene *sll0506* (encoding for undecaprenyl phosphate synthetase), because the *sll0505* gene overlaps with *sll0506* and is predicted to contain a possible promoter region for *sll0506* (*17*). However, we only achieved partial segregation by both attempts (fig. S3). In contrast, complete segregation was obtained in the background of glucose-tolerant *Synechocystis* strain (GT-strain), as revealed by the absence of the wild-type (WT) gene fragment through polymerase chain reaction (PCR) amplification (fig. S3). This implies that DacA is not essential for the viability of the GT-*Synechocystis* under standard, glucose-free conditions but it is, for unknown reasons, essential for the lifestyle of GS-*Synechocystis*. Unless mentioned otherwise, the following results were generated using the fully segregated Δ*dacA* insertion mutant in GT-*Synechocystis* background. However, we were able to reproduce all these results using the Δ*dacA* deletion mutant in GT-*Synechocystis* as well.

Measurements of the intracellular c-di-AMP concentration confirmed that the completely segregated Δ*dacA* mutant was free of c-di-AMP, while the WT cells contained around 4.6 μmol per cell of c-di-AMP under photoautotrophic growth conditions (Fig. 2A). To further confirm that *dacA* gene (*sll0505*) encodes an active di-adenylate cyclase able to synthesize c-di-AMP, *Escherichia coli*, which does not synthesize c-di-AMP naturally, was transformed with a plasmid expressing a *sll0505*–green fluorescent protein (GFP) fusion protein under the control of the isopropyl-β-D-thiogalactopyranoside (IPTG)–inducible T7 promoter. High concentration of c-di-AMP was detected in *E. coli* cells upon induction as compared to un-induced cells (fig. S3), confirming the annotation of DacA.

In cyanobacteria, c-di-AMP signaling was previously linked to osmoregulation, to the resuscitation from long-term chlorosis under nitrogen starvation condition, and to day-night rhythms (*11*, *17*, *19*), whereas SbtB was shown to be important for C_i acclimation (*20*). It was therefore obvious to assume that c-di-AMP perception by SbtB could be involved in one or more of those c-di-AMP–linked processes by comparing the phenotypes of the mutants Δ*dacA* and Δ*sbtB* under different growth conditions.

First, *Synechocystis* WT, Δ*dacA*, and Δ*sbtB* mutants were subjected to osmotic stress by treating them with increasing concentrations of sorbitol (50 to 600 mM) (fig. S4). In agreement with a previous study (*17*), the growth of Δ*dacA* was strongly impaired in the presence of high osmolyte concentrations, with 300 mM sorbitol completely preventing growth. By contrast, the Δ*sbtB* mutant was not affected by osmotic stress (fig. S4), implying that c-di-AMP sensing by SbtB is not involved in osmoregulation. This clear phenotype of Δ*dacA* supports the notion that c-di-AMP has a key role in osmoregulation and maintenance of the intracellular turgor pressure within cyanobacteria. Moreover, this phenotype agrees with the identification of several ion and osmolyte transporters in the c-di-AMP pull-down experiment, including those for K^+, Na^+, and Mg^{2+} ions, glutamate, and maltose (Fig. 1B).

Second, the recovery from nitrogen starvation–induced chlorosis of the mutant strains was tested by resupplementation with a nitrogen source. The Δ*dacA* mutant was neither able to properly enter chlorosis nor to recover from chlorosis nearly as efficiently as the WT cells, which is consistent with high expression of the *dacA* gene under resuscitation conditions (fig. S5) (*19*). In contrast, the Δ*sbtB* mutant did not show any phenotypic difference to WT during these treatments (fig. S5). This suggests that SbtB is not required for entering and exiting from chlorosis, whereas c-di-AMP plays an important role in this process perhaps due to interaction with as yet unknown receptor protein.

Third, we wanted to test whether c-di-AMP might be involved in primary C_i acquisition, because our previous study revealed that Δ*sbtB* is impaired in proper C_i acclimation (*20*). Therefore, the photosynthetic HCO_3^--dependent oxygen evolution of the Δ*dacA* mutant was compared to WT in high C_i (HC)– and low C_i (LC)–acclimated cells (Fig. 2B and fig. S6). Both WT and Δ*dacA* cells showed the expected acclimation to HC conditions by lowering affinity for HCO_3^- as estimated by an increase of HCO_3^- K_m to about 300 μM (Fig. 2B). Under LC conditions, the affinity toward HCO_3^- increased markedly in both Δ*dacA* mutant and WT cells (Fig. 2B). Although the initial rise of the photosynthetic activity at low C_i concentrations was similar, the maximal photosynthetic rates (V_{max}) in the Δ*dacA* mutant was lower than in WT cells under LC-acclimated condition. The decreased V_{max} indicates a lower activity of the Calvin-Benson cycle (fig. S6), at saturating C_i amounts. Despite this difference, this experiment indicated that, in contrast to the Δ*sbtB* mutant, operation of the CCM was not affected in the Δ*dacA* mutant (*20*).

Last, we investigated the involvement of DacA and SbtB in diurnal growth by exposing the cells to 12-hour light/12-hour dark cycles. Similar to *S. elongatus* (*11*), the *Synechocystis* Δ*dacA* mutant showed a strong growth defect under day-night conditions (Fig. 2, C and D, and fig. S7). Unexpectedly, the Δ*sbtB* mutant showed a similar diurnal growth impairment (Fig. 2, C and D, and fig. S7). SbtB is known to regulate the HCO_3^- transporter SbtA through direct protein-protein interaction in response to the energy state of the cell and the second messenger cAMP (*20*, *22*, *23*, *27*), raising several questions of either an involvement of SbtA or cAMP in impaired

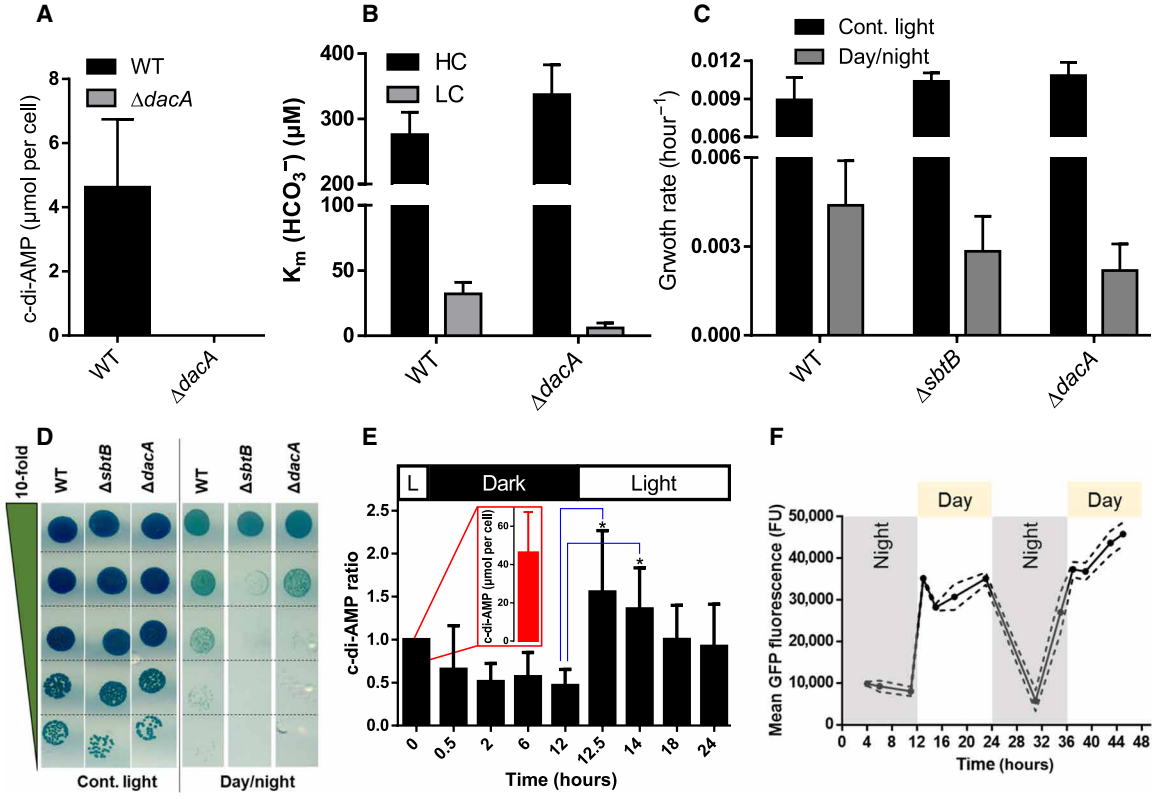

Fig. 2. Physiological characterization of Δ*sbtB* and Δ*dacA* mutants. (**A**) c-di-AMP concentration shown in μmol per cell within vegetative photoautotrophic growing *Synechocystis* sp. PCC 6803 WT (black bar) and the di-adenylate cyclase deficient mutant Δ*dacA* (gray bar; undetectable). (**B**) Bicarbonate affinity represented by the K_m (HCO_3^-) values of *Synechocystis* WT and the Δ*dacA* mutant under either high carbon (HC; black bars) or low carbon (LC; gray bars) regimes. (**C**) Specific growth rate of *Synechocystis* WT, Δ*sbtB*, and Δ*dacA* cells under either continuous light (black bars) or a 12-hour diurnal rhythm (gray bars). (**D**) Growth test by drop plate assay of *Synechocystis* WT, Δ*sbtB*, and Δ*dacA* cells as indicated under either continuous light (left) or a 12-hour diurnal rhythm (right). Cells were normalized to an optical density at 750 nm (OD_{750}) of 1.0 and serial diluted in 10-fold steps (top to bottom; depicted by a green triangle). (**E**) Relative c-di-AMP concentration within *Synechocystis* WT cells throughout a 12-hour diurnal rhythm. Statistically significant differences ($P < 0.05$) are indicated by asterisk (*) for the transition from the end of the night phase (12 hours) to early day-phase (12.5 and 14 hours). Values are means ± SD; $n = 5$ to 6 independent measurements. The c-di-AMP was not detectable within Δ*dacA* cells. The *x* axis shows the time in hours; the *y* axis shows the relative amount of c-di-AMP normalized to the first time point at the end of the day phase (indicated by 0.0 hours). (E) Inset: c-di-AMP concentration shown in micromoles per cell for the first measurable time point (0.0 hours). (**F**) Mean of in vivo SbtB-sfGFP expression throughout a 12-hour diurnal rhythm, as indicated. The *x* axis shows the time in hours; the *y* axis shows the mean GFP fluorescence in fluorescence units (FU).

diurnal growth. However, the Δ*sbtA* and Δ*cya1* (encodes for the major cAMP cyclase in *Synechocystis*) mutants grew almost like WT cells under 13 successive day-night cycles (fig. S7D). Together, these results indicated that the common growth defect of the Δ*sbtB* and Δ*dacA* mutants under diurnal cycles (Fig. 2, C and D) was not mediated by neither cAMP nor by a defect in primary C_i acquisition via SbtA (Figs. 2B and figs. S6 and S7). Rather, it pointed toward a specific/unidentified c-di-AMP–controlled process, involving signal perception by SbtB.

Diurnal cycling of c-di-AMP correlates with SbtB

To gain insight into the mechanism that makes c-di-AMP and SbtB indispensable for diurnal growth, we first looked for *sbtB* (*slr1513*) and *dacA* (*sll0505*) expression in the transcriptome dataset of diurnally grown *Synechocystis* cells (*30*). Both *sbtB* and *dacA* transcripts showed a diurnal dynamic, with a sharp increase at the beginning of the day and a decline in the dark phase (fig. S8). To reveal whether the changes in *dacA* transcript levels correlated with the c-di-AMP levels, the intracellular concentration of c-di-AMP was determined in WT *Synechocystis* cells under diurnal growth at different time points during day-night cycles. The first sampling point was taken at the end of the light phase, and four samples were taken during the following 12 hours of dark phase and four samples in the following 12 hours of light phase (Fig. 2E). While the c-di-AMP concentration dropped during the dark period, a rapid two to fourfold increase in c-di-AMP concentration was observed 30 min after onset of light (Fig. 2E). The maximum c-di-AMP concentration was reached in the early light phase and then declined throughout the remaining light phase (Fig. 2E), correlating well with the expression pattern of *dacA* (fig. S8). Because SbtB is known to bind the second messenger cAMP as well and to further exclude any possible role for cAMP in day-night metabolism (fig. S7E), we checked for intracellular concentration of cAMP under the same cycling condition in the WT and Δ*dacA* cells. The intracellular concentration of cAMP did not change markedly between day-night cycle within both of WT and Δ*dacA* cells (fig. S8C), which further supports the specificity of c-di-AMP in regulating *Synechocystis* diurnal metabolism. Moreover, we monitored SbtB expression using as a reporter the fluorescently

labeled fusion protein SbtB–super-folded GFP (sfGFP) (*20*). The SbtB-sfGFP fluorescence showed the same cycling pattern as the c-di-AMP concentration, dropping during the dark phase and peaking during the day (Fig. 2F). Last, to examine whether there might be a regulatory connection between *sbtB* and *dacA* at the level of transcription, we checked for the expression profile of *sbtB* (*slr1513*) in Δ*dacA* and for *dacA* (*sll0505*) in Δ*sbtB* mutant in comparison to WT cells using microarray technology (fig. S8, D and E). The *sbtB* mutation had negligible effect on the expression of *dacA*, while the *dacA* mutation led to partial down-regulation of *sbtB*, which could explain the inability of *dacA* mutant to fully activate the Calvin-Benson cycle (fig. S6), consistent with the proposed role for SbtB in regulating the entire CCM (*20*). Notably, the expression of the genes situated upstream (*sll0504*) and downstream (*sll0506*) of *dacA* was similar in both the Δ*dacA* and Δ*sbtB* mutants and very close to that of the WT cells, which confirmed that *dacA* mutation has no polar effects on the transcription of neighboring genes.

SbtB regulates glycogen metabolism via interaction with the glycogen-branching enzyme GlgB

Because the proteins of the PII superfamily, to which SbtB belongs, are known to exert their regulatory functions via direct protein-protein interaction (*29*), we hypothesized that SbtB binds to yet unknown target(s) in a c-di-AMP–dependent manner, thereby affecting diurnal growth.

To identify potential SbtB interaction partners, we characterized the global SbtB interactome using several mass spectrometry-based pull-down approaches and screened for hits that could be involved in day-night acclimation. First, coimmunoprecipitation (CoIP) experiments were performed with WT *Synechocystis* crude cell extracts using α-SbtB–specific antibodies. As negative control, we used crude cell extracts from Δ*sbtB* cells. Compared to the negative control, the immunoprecipitate contained five to ninefold enriched enzymes related to glycogen metabolism (fig. S9A). In particular, we identified glycogen synthase (GlgA2, *sll1393*), glycogen phosphorylase (GlgP2, *slr1367*), glycogen-branching enzyme (GlgB, *sll0158*), and glycogen-debranching enzyme (GlgX1, *slr0237*) as potential SbtB interacting partners. Because glycogen metabolism is of primary importance for day-night acclimation in cyanobacteria (*3*, *8*), the observed enrichment of glycogen metabolic enzymes would fit into the proposed c-di-AMP–related function of SbtB in diurnal growth.

To further elucidate c-di-AMP–dependent SbtB interactions, we performed several pull-down assays by immobilizing recombinant C-terminal His_8- or strep-tagged *Sc*SbtB protein on Ni^{2+} magnetic beads or streptavidin magnetic beads, respectively, and incubating them with *Synechocystis* crude cell extracts either in the presence or absence of c-di-AMP, followed by successive washes to remove the unbound proteins. In several pull-down experiments, the known SbtB-target SbtA was identified, which validated the procedure. With the His_8-tagged *Sc*SbtB protein on Ni^{2+} magnetic beads, in addition to SbtA, we identified again GlgA2, GlgP2, GlgB, GlgX, and furthermore the second glycogen-debranching enzyme (GlgX2, *slr1857*) and glucose-1-phosphate adenylyltransferase (GlgC, *slr1176*). Notably, GlgB and GlgA2 were more than 20-fold enriched in the presence of c-di-AMP (fig. S9B), implying that they could be of particular importance. When strep-tagged *Sc*SbtB protein was used as affinity bait, a cleaner pull-down with a low background due to higher specificity of streptavidin beads was obtained. Using this attempt, only the glycogen-branching enzyme GlgB was enriched as specific interaction partner (Fig. 3A and fig. S9, C and D). In the presence of c-di-AMP, GlgB was 14 times more abundant as compared to the pull-down in the absence of effector molecules (Fig. 3A). This enrichment was specific for c-di-AMP and not observed in the presence of cAMP (fig. S9, C and D). GlgB was not identified in the negative control (empty streptavidin beads) as well.

To further validate the specificity of SbtB-GlgB interaction and examine possible interactions with other glycogen-related enzymes by an independent method, we carried out interaction assays using the bacterial adenylate cyclase two-hybrid (BACTH) system. The BACTH system relies on the reconstitution of a functional adenylate cyclase (Cya) upon positive interaction of the proteins of interest fused to the T25 and T18 subunits of Cya, which can be detected by color change on X-Gal reporter plates. Here, we fused the T25 subunit of Cya N-terminally to SbtB, while the T18 subunit of Cya was fused either N- or C-terminally to the glycogen-related enzymes GlgA1, GlgA2, GlgP1, GlgP2, GlgB, and GlgC (fig. S10). The T25-SbtB fusion with an empty pUT18 vector was used as negative control, while the leucine zipper interaction was used as positive control. A clear interaction was observed only between T25-SbtB and GlgB N-terminally tagged with a T18 subunit (Fig. 3B), whereas no interaction was obtained with C-terminally tagged GlgB and the other glycogen metabolic enzymes (fig. S10). This result strongly indicated that SbtB is a specific interactor of GlgB.

To gain further insights into SbtB-GlgB complex formation, we studied the SbtB-GlgB interaction using microscale thermophoresis (MST). We titrated SbtB against labeled GlgB in the presence or absence of c-di-AMP. SbtB was able to bind GlgB with a K_d of 0.22 ± 0.07 μM (Fig. 3C); however, the presence of c-di-AMP (100 μM) did not change the binding constant markedly (K_d of 0.43 ± 0.10 μM).

Molecular basis for diurnal, c-di-AMP–dependent control of GlgB by SbtB

The photosynthetic synthesis of glycogen as carbohydrate reserve during the day is crucial for cyanobacterial survival in the night (*3*, *7*, *31*). To confirm the involvement of GlgB in this process, we tested diurnal growth of a Δ*glgB* mutant. The Δ*glgB* mutant was impaired in diurnal growth in a similar manner to the Δ*sbtB* and Δ*dacA* mutants (Fig. 3D), confirming the importance of glycogen metabolism and GlgB in diurnal growth. To obtain further evidence of a functional link between SbtB and the regulation of glycogen metabolism via GlgB in a c-di-AMP–dependent manner, we determined the intracellular glycogen concentration at the mid of the day phase. As compared to *Synechocystis* WT cells, glycogen levels were significantly reduced in all three mutants (Δ*sbtB*, Δ*dacA*, and Δ*glgB*) (Fig. 3E), with Δ*dacA* showing the lowest amount of glycogen with about 14.7%, Δ*sbtB* with 28.2%, and Δ*glgB* with 26.7% (Fig. 3E). Complementation of Δ*sbtB* by introducing copy of *slr1513* under the control of the *psbA2* promoter restored the growth of the mutant under day-night rhythm and restored the glycogen content to the levels of WT cells (fig. S11, A and B). Moreover, addition of glucose to BG_{11} medium rescued the diurnal growth defect of Δ*sbtB* (fig. S11C).

Because glycogen catabolism is the major source for respiration in the dark, supporting a heterotrophic mode of metabolism (*32*), we measured oxygen evolution and respiration during three successive day-night cycles. During the day, both Δ*sbtB* and Δ*dacA* mutants showed 50% less oxygen evolution than WT cells (Fig. 3F), in agreement with the inability of both mutants to fully activate the

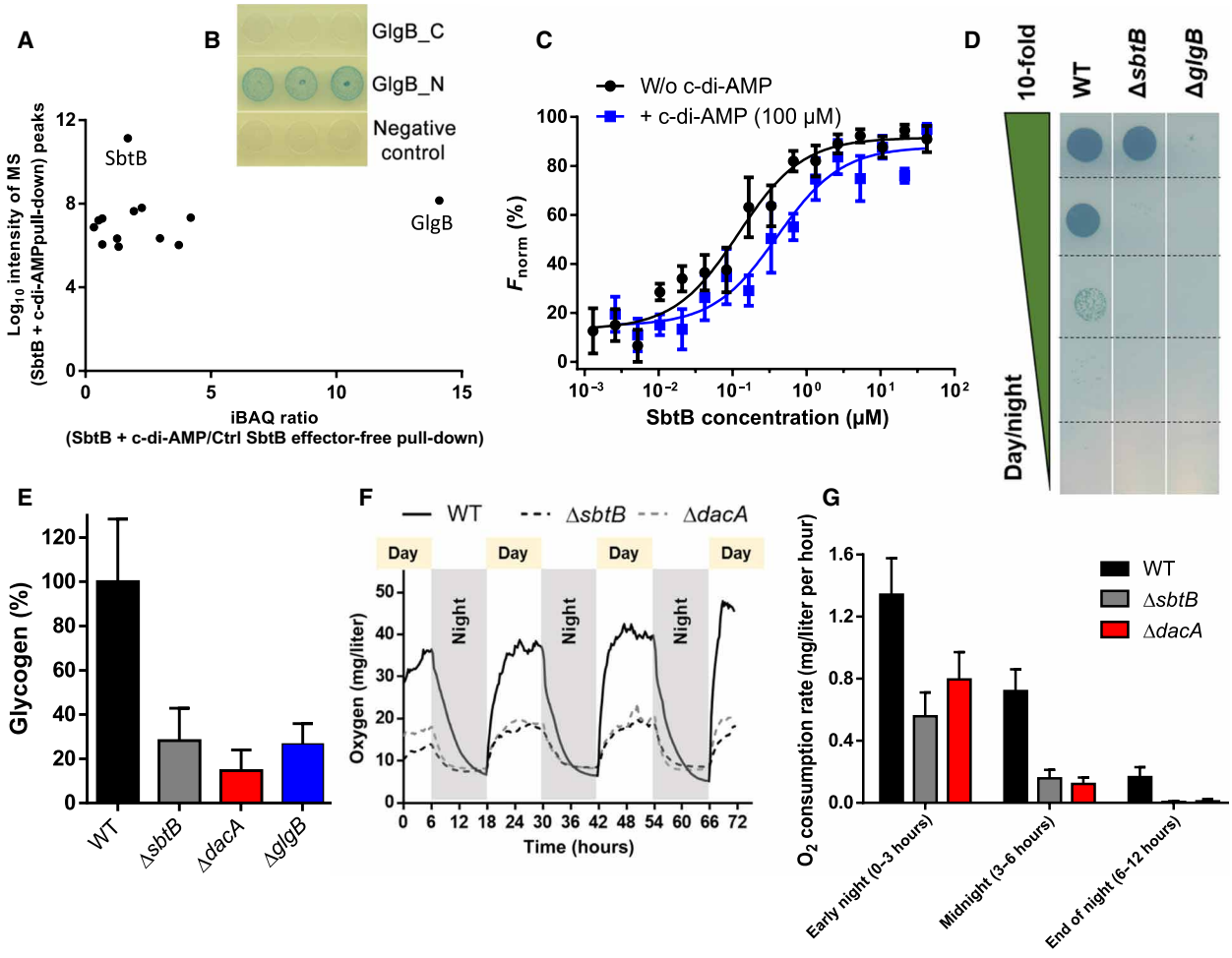

Fig. 3. Regulation of glycogen metabolism via c-di-AMP dependent SbtB signaling. (**A**) Streptavidin magnetic bead-based pull-downs using strep-tagged *Sc*SbtB protein in the absence or presence of c-di-AMP. The c-di-AMP enriched SbtB-GlgB interaction. (**B**) BACTH assay was performed using *E. coli* cells expressing T25-SbtB fusion together with either C-terminal (GlgB_C) or N-terminal (GlgB_N) T18-GlgB fusion, or empty Cya-T18 (negative control). SbtB-GlgB interaction is evidenced by appearance of a blue color on X-Gal reporter plates (middle). (**C**) MST analysis of the SbtB-GlgB interaction in either presence (blue line) or absence (black line) of 100 µM c-di-AMP, as indicated. The *y* axis shows the relative, normalized fluorescence units. (**D**) Growth test by drop plate assay of *Synechocystis* WT, Δ*sbtB*, and Δ*glgB* cells, as indicated in a 12-hour diurnal rhythm. Cells were normalized to an OD_{750} of 1.0 and serial diluted in 10-fold steps (up to down). (**E**) Relative glycogen levels of *Synechocystis* WT (black bar), Δ*sbtB* (gray bar), Δ*dacA* (red bar), and Δ*glgB* (blue bar) cells in the midday of a 12-hour diurnal rhythm. The glycogen content was normalized to 100% of WT cells. (**F**) Photosynthetic oxygen production and respiration of *Synechocystis* WT (black line) in comparison to Δ*sbtB* (black, dashed line) and Δ*dacA* (gray, dashed line) throughout a 12-hour diurnal rhythm for 72 hours, as indicated. The *y* axis shows the oxygen levels in parts per million (milligrams per liter). (**G**) Oxygen consumption rates in milligrams per liter per hour based on the data from (F). Oxygen consumption rates for WT (black bars), Δ*sbtB* (gray bars), and Δ*dacA* (red bars) were calculated for the early night (first 3 hours), midnight (next 3 to 6 hours), and the end of the night (last 6 to 12 hours).

Calvin-Benson cycle (fig. S6) (*20*). Upon onset of darkness, all strains started respiration, with WT cells displaying approximately twofold higher oxygen consumption than the mutants. Whereas WT cells kept on the respiration process for the whole night (12 hours), the Δ*sbtB* and Δ*dacA* cells ceased respiration after 6 hours (fig. 3FG). This result suggests that both mutants were unable to maintain respiration throughout a 12-hour night period and, therefore, were impaired in diurnal growth. To confirm this assumption, we determined the viability of the mutants compared to the WT cells during a prolonged dark incubation for 5 days. As revealed by drop plate assay, both mutants showed a marked loss of viability after 2 days of darkness. After 5 days of darkness, Δ*sbtB* cells were completely unviable (fig. S11D). Moreover, all strains retained a comparable efficiency of photosystem II (PSII) and photosynthetic pigmentations over 3 days of darkness, implying that the loss of viability of the mutants was not due to an alteration in the photosynthetic machinery (fig. S11, E and F). Again, all of those results indicate that the low glycogen levels in both mutants are the main cause of the growth defect under the day-night rhythm. However, it should be mentioned that Δ*dacA* cells showed about 25% reduction of apparent PSII quantum yield [determined by pulse-amplitude modulation (PAM) fluorescence] in the absence of actinic light as compared to WT cells (fig. S11E).

DISCUSSION

Here, we revealed that the PII-like signaling protein SbtB binds the second messenger c-di-AMP in addition to the standard adenine

nucleotides (AMP, ADP, and ATP) and to the carbon status reporting second messenger nucleotide cAMP. To our knowledge, this is the first signaling protein known to interact with both cAMP and c-di-AMP. This highlights the central role of SbtB as a switch point in cyanobacterial cell physiology, integrating not only signals from the energy state and carbon supply through adenine nucleotide and cAMP binding (*20*, *23*, *27*), respectively, but also from the diurnal state by binding to c-di-AMP. We were able to confirm the ability of SbtB to bind c-di-AMP from two distinct cyanobacterial species of unicellular *Synechocystis* sp. PCC 6803 and filamentous filamentous *Nostoc* sp. PCC 7120, which emphasizes a general role for c-di-AMP signaling via SbtB. In Gram-positive bacteria, c-di-AMP synthesis is related to cell wall homeostasis, potassium homeostasis, and osmotic control (*12*–*14*). Previous data indicated that, in cyanobacteria too, c-di-AMP might also control osmoregulation (*17*), which we were able to confirm in our study as well (Fig. 1B). We linked the c-di-AMP signaling with cyanobacterial osmoregulation by identifying several c-di-AMP target transporters in the c-di-AMP–dependent pull-down experiment, including transporters for K^+, Na^+, and Mg^{2+} ions, glutamate, and maltose. Furthermore, a link between c-di-AMP and nighttime survival was reported in *S. elongatus* as suggested by loss of viability of the Δ*dacA* mutant under dark conditions by a cryptic mechanism (*11*). Here, we revealed the exact mechanism by which c-di-AMP contributes to the regulation of the day-night rhythm in cyanobacteria.

Our data indicate that binding of c-di-AMP to SbtB modulates the interaction of SbtB with enzymes of glycogen synthesis, particularly with the glycogen-branching enzyme GlgB (Fig. 4), which we were able to confirm by different independent methods. In the *sbtB*-deficient mutant, the accumulation of glycogen during daytime is severely diminished and to a similar degree in the Δ*dacA* or Δ*glgB* mutants, which are unable to synthesize c-di-AMP or branched glycogen, respectively. Further support for a correlation between c-di-AMP concentration and glycogen synthesis comes from the diurnal cycling of c-di-AMP concentration, high during the day, when glycogen is synthesized, and low in the night, when glycogen is consumed. In *Synechocystis*, the daily c-di-AMP cycling levels correlate well with the expression of the diadenylate cyclase-encoding gene *sll0505* (*dacA*) under day-night cycles. In agreement, the SbtB-encoding gene *slr1513* was found to follow the same expression pattern as *sll0505* (*30*). Furthermore, the interaction between SbtB and GlgB was enriched in the presence of c-di-AMP, at least in the in vivo pull-down experiments; however, such influence was not observed using the recombinant purified proteins from *E. coli* in the in vitro MST experiment. The reason for that is presently ambiguous, but one possibility is that other components in the *Synechocystis* crude extract contribute to enhancing the affinity of SbtB for GlgB, perhaps other components of the glycogen metabolic enzymes, such as GlgA2 and/or GlgP2. Of note, GlgA2 and GlgP2 were enriched in the CoIP and His-tag SbtB pull-downs; however,

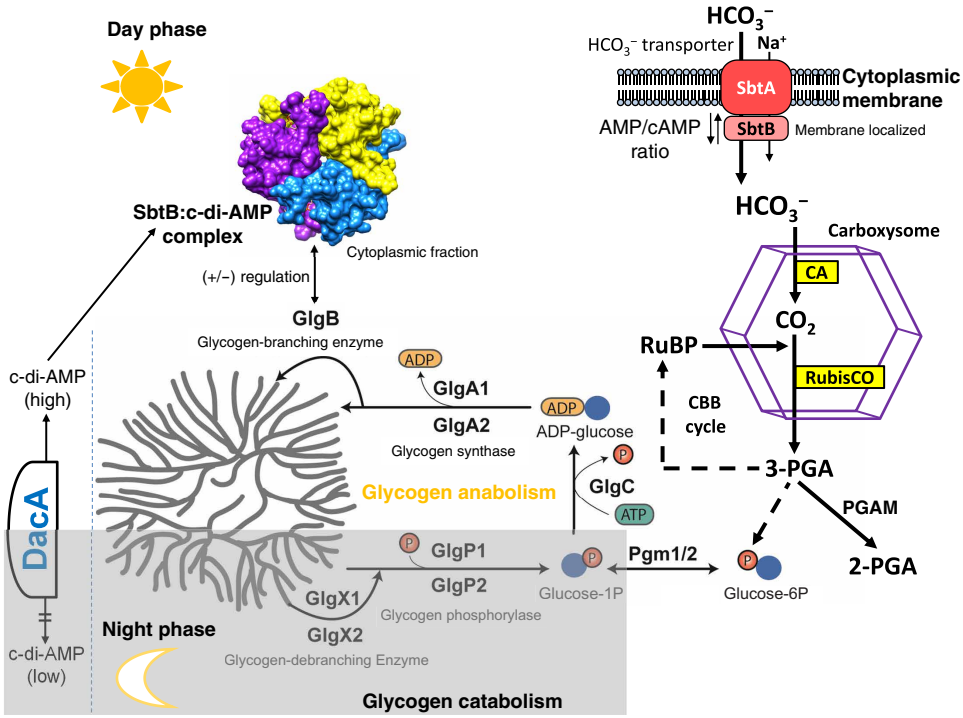

Fig. 4. Model of regulation of day-night switch of glycogen metabolism via c-di-AMP sensing by SbtB. During the day, cyanobacteria use an active carbon concentrating mechanism, which composes of several C_i uptake systems (among them the HCO_3^- transporter SbtA), and the carboxysome, where HCO_3^- is dehydrated to CO_2 by carbonic anhydrase (CA) and then CO_2 fixation occurs by RubisCO. Via the activity of Calvin-Benson (CBB) cycle, a part of the newly fixed carbon is redirected toward synthesis of carbon storage compound (glycogen). Simultaneously, the concentration of the second messenger nucleotide c-di-AMP increases in the day due to di-adenylate cyclase (DacA) activity. The soluble fraction of SbtB protein, not sequestered by SbtA, interacts with c-di-AMP and promotes glycogen synthesis by interacting with the glycogen-branching enzyme GlgB. After nightfall, c-di-AMP concentration decreases, and the catabolism of glycogen, which produced in the day, is the resource for nighttime survival.

we were not able to confirm such interaction with BACTH, implying that they could be indirectly involved in modulating SbtB-GlgB interaction. Nevertheless, a genome-wide fitness assessment of *S. elongatus* revealed that mutations in genes encoding for GlgB (*Synpcc7942_1085*) and SbtB (*Synpcc7942_1476*) and, to a less extent, for DacA (*Synpcc7942_0263*) cause a strong decrease in the bacterium fitness under diurnal rhythms (*3*) but not for SbtA (*Synpcc7942_1475*) or the putative cAMP synthases (*Synpcc7942_2195* or *Synpcc7942_0663*), which further support the specificity notion of SbtB and c-di-AMP signaling for the fitness of cyanobacterial diurnal metabolism.

However, c-di-AMP concentration oscillated in the opposite direction in *S. elongatus*, with high concentration in the night and low concentration during the day (*11*). The reasons for the discrepancy are now unclear, although both strains show a clear phenotypic defect under diurnal rhythm in the absence of the c-di-AMP cyclase, confirming the essentiality of c-di-AMP for cyanobacterial growth under day-night rhythm. It is known that *S. elongatus* uses a precisely operating circadian clock machinery to tune metabolism in a diurnal manner (*1*, *3*, *8*). Although components of this clock are conserved in *Synechocystis*, the overall process appears to be distinct owing to the emergence of multiple paralogs of the oscillator proteins (*6*, *33*). However, to comprehensively understand the control of the diurnal cycling of SbtB and c-di-AMP concentration, detailed analysis of the clock influence on SbtB and on c-di-AMP specific cyclase and phosphodiesterase activities is required. Notably, *sbtB* expression was strongly deregulated in the mutant of the circadian clock output regulator RpaA (*6*), which cannot survive the day-night rhythm as well (*8*).

In contrast to Δ*sbtB* (Fig. 3E), the Δ*rpaA* mutant is not impaired in glycogen synthesis during daytime (*8*, *34*). In this case, the inability of Δ*rpaA* to grow under day-night regime is due to the failure of this mutant to activate, in the night, carbon catabolic genes, including components of the OPP pathway, glycolysis, and glycogen degradation via GlgP (*1*, *6*, *8*, *34*). Apparently, SbtB and RpaA are working in opposite directions on glycogen anabolism and catabolism, respectively. Nevertheless, it appears that RpaA is involved in regulation of *sbtB*-gene expression in the day phase by yet unknown mechanism (*6*).

In addition to a role in regulating glycogen synthesis, c-di-AMP appears to regulate numerous ion transporters and osmotic responses, as deduced from the identification of several K^+ transporters, including KtrA (*sll0493*), TrkA (*slr0773*), and MthK (*sll0993*) as c-di-AMP targets. This highlights a conserved role for c-di-AMP in controlling osmotic homeostasis and K^+ transport (*12*–*14*), which is of particular importance, since K^+ is the major inorganic cation in the cytoplasm, acting as counter-ion of glutamate. In agreement with our identification of KtrA as a potential c-di-AMP target, the Na^+-dependent K^+ uptake system KtrABE was previously shown to be required for regulation of cell turgor and the adaptation to hyperosmotic stress elicited by either sorbitol or NaCl (*35*, *36*). However, osmotic control by c-di-AMP appears to act independently of SbtB, because the Δ*sbtB* mutant was not impaired in its responses to osmotic stress conditions like Δ*dacA* (fig. S4). Moreover, it seems also that the Mg^{2+} transporter MgtE is a conserved c-di-AMP target among different bacterial phyla (*12*, *14*, *28*). Of note, Mg^{2+} is of particular importance for the photosynthetic lifestyle of cyanobacteria as it is the central ion in the chlorophylls and required for the maintenance of the thylakoid membranes (*37*).

Cross-talk between second messenger nucleotides is perhaps a more common phenomenon than so far realized. Recently, it was found that the second messengers c-di-GMP and (p)ppGpp reciprocally control *Caulobacter crescentus* growth by competitive binding to a metabolic switch protein, SmbA (*38*). With this in mind, SbtB might play a similar role in cyanobacterial physiology. As is typical for signaling proteins of the PII family (*29*, *39*), SbtB seems to simultaneously perform multiple tasks in controlling cyanobacterial carbon metabolism: controlling bicarbonate uptake via SbtA interaction in response to cAMP and energy state of the cell (*20*, *22*, *23*, *27*) and controlling glycogen synthesis via interaction with glycogen-branching enzyme GlgB in response to c-di-AMP. Accordingly, SbtB would link the control of glycogen synthesis to bicarbonate availability. Under low carbon conditions, SbtB was preferentially found associated to the membrane fraction, presumably due to binding to SbtA (*20*, *23*). Thereby, less SbtB would be available for activation of glycogen synthesis, which takes place in the cytoplasmic space. More SbtB would become available under elevated C_i conditions, when SbtB is enriched in the soluble fraction (*20*). This hypothesis agrees with the fact that the glycogen levels in cells grown under atmospheric CO_2 concentration are low but increase at elevated C_i conditions (*40*, *41*). But, apparently, SbtB integrates the cellular information of both second messengers c-di-AMP and cAMP independently of each other, in agreement with distinct phenotype of Δ*dacA* and Δ*cya1* mutants (fig. S7). Whereas, cAMP acts as an indicator for cellular carbon status (*20*, *26*) and c-di-AMP is a specific indicator of day-night transition (Fig. 2E), and possibly they compete for SbtB available sites. The fact that c-di-AMP binding to SbtB affects the conformation of the T-loop is in perfect agreement with this scenario. The T-loop represents the major protein-interaction motif of PII signaling proteins (*39*). In complex with c-di-AMP, we have found the T-loop in a new conformation that is distinct from the cAMP or linear adenine nucleotide complex forms (Fig. 1E and fig. S2), a conformation that is seemingly driving the interaction with the newly identified GlgB and possibly yet to be identified receptors. The precise structural and regulatory mechanisms of these interactions, especially between SbtB:c-di-AMP and GlgB, await further biochemical and structural elucidation.

MATERIALS AND METHODS

Generation and purification of recombinant proteins

All the plasmids and primers used in this study are listed in (table S1). The recombinant C-terminal StrepII-tagged *Sc*SbtB was expressed and purified as previously described (*20*). Recombinant C-terminal StrepII-tagged SbtB protein from the filamentous *NsSbtB* was constructed as described in (*20*) using the primer pairs compatible for *Ns*SbtB. For generation of recombinant C-terminal His_8-tagged *Sc*SbtB, the SbtB encoding gene *slr1513* was amplified from *Synechocystis* sp. PCC 6803 and inserted via Gibson cloning in linearized pET28a vector. For generation of recombinant N-terminal His_6-tagged GlgB, the GlgB encoding gene *sll0158* was amplified from *Synechocystis* sp. PCC 6803 and inserted via Gibson cloning in linearized pET15b vector. The recombinant StrepII-tagged proteins were purified as previously described (*20*, *24*), while the His-tagged proteins were purified as described previously (*24*, *42*). For the recombinant C-terminal GFP-tagged DacA, which was used for quantification of c-di-AMP in *E. coli*, the DacA encoding gene

sll0505 was amplified from *Synechocystis* sp. PCC 6803 and inserted via Gibson cloning in linearized pET28a-eGFP–based vector.

Crystallization, crystal handling, data collection, and structure elucidation

For soaking experiments, crystals of the trigonal apo crystal form were reproduced as described previously (*20*). These crystals were grown with a reservoir solution composed of 0.1 M phosphate-citrate (pH 4.2) and 40% (w/v) polyethylene glycol (PEG) 300 and were soaked in a droplet of reservoir solution supplemented with 0.33 mM c-di-AMP (cyclic di-3′,5′-adenylate sodium salt; catalog no. C088, BioLoG, Germany) for 4 hours. For cocrystallization, 2.5 mM c-di-AMP was added to the protein solution, and crystallization trials were performed as described (*20*). Cocrystals were grown with a reservoir solution of 0.1 M tris-sodium citrate (pH 5.6), 10% (w/v) PEG 4000, and 10% (w/v) isopropanol, and 20% PEG 400 was used for cryo-protection. All crystals were flash-cooled in liquid nitrogen, and diffraction data were collected at 100 K on a PILATUS 6M-F detector at beamline X10SA of the Swiss Light Source (PSI, Villigen, Switzerland). All data were indexed, integrated, and scaled using the XDS software package (*43*). The structures were solved using difference Fourier methods based on the trigonal apo-*Sc*SbtB structure (PDB: 5O3P). After initial rigid body refinement with REFMAC5 (*44*), it became apparent that the cocrystal structure was essentially identical to the costructure obtained by soaking and not regarded further. The structure of the *Sc*SbtB:c-di-AMP complex was rebuilt and completed by cyclic manual modeling with Coot program and refinement with REFMAC5 based on the data obtained from the soaking experiment. Data collection and refinement statistics are shown in (table S2). Structural representations were prepared using UCSF Chimera.

Generation of mutants

The nonmotile unicellular, freshwater cyanobacterium *Synechocystis sp*. PCC 6803 (glucose-tolerant Tübingen substrain; called here GT-strain) was used as a reference WT strain in this study. Our laboratory "Tübingen" substrain of the glucose-tolerant WT *Synechocystis sp*. PCC 6803 is originally derived from the parental strain *Synechocystis sp*. PCC-M (*45*). While the glucose-sensitive strain of *Synechocystis* sp. PCC 6803 (called here GS-strain) was obtained from Rostock cyanobacterial culture collection and adapted to grow under our standard cultivation conditions in Tübingen for almost 14 years. All constructs used in this study were generated via Gibson assembly, unless specified otherwise. All knockout mutants were generated with homolog recombination using the natural competence of *Synechocystis* sp. PCC 6803, as described previously (*20*). All plasmids and primers used in this study are listed in (table S1).

For generation of knockout deletion mutants in either GT-strain or GS-strain, the mutants were constructed by deleting the ORFs *slr1513*, *sll0505*, and *sll0158* (designated *sbtB*, *dacA*, and *glgB*, respectively) and replaced with the erythromycin, spectinomycin, and chloramphenicol resistance cassette, respectively. The cAMP-free mutant was created by knocking out *slr1991* (designated Δ*cya1*), which encodes the soluble adenylyl cyclase in *Synechocystis sp*., as described previously (*20*). For the generation of the *sbtA* knockout mutant, the *sbtA* upstream sequence was obtained using the primer combination SbtAB_Apa5 and DelSbtA_Bam5, whereas the *sbtA* downstream sequence was obtained using the primer combination SbtAB_Sac3 and DelSbtA_Bam3. First, the two fragments were cloned each in a single pGEMT vector (Promega), and then, the two fragments were combined into one vector by transferring the downstream fragment as Sac I/Bam HI fragment into the vector containing the upstream fragment. Into the central Bam HI restriction site, either a kanamycin or a streptomycin resistance cassette was inserted. The Δ*dacA* insertion mutant was generated by inserting a kanamycin resistance cassette into the region encoding for the active center of DacA. All the plasmids used to generate the mutants were verified by sequencing and then transformed in *Synechocystis* sp. PCC6803, as described (*20*). All mutants were selected on BG_{11} plates supplemented with proper antibiotics and verified by PCR.

For complementation, SbtB-sfGFP strain was generated by introducing the *sbtB* gene (*slr1513*) fused to the gene encoding sfGFP under the control of the native promoter of *sbtB* gene into Δ*sbtB* backgrounds using the self-replicating plasmid pVZ322, as described previously (*20*). For inducible complementation of Δ*sbtB*, the *sbtB* gene (*slr1513*) was reinserted in the genome under the control of the light inducible promotor *psbA2*.

Cultivation conditions

All cyanobacterial growth experiments were performed in nitrate supplemented BG_{11} medium (BG_{11}^{n}) with addition of 5 mM $NaHCO_3$ to avoid C_i limitation. Precultures were grown in shaking conditions at 28°C under continuous light (~50 μE) until mid of logarithmic growth phase before each experiment started. Cells were always normalized to their optical density at 750 nm using a Helios Gamma UV-Vis Spectrophotometer (Thermo Fisher Scientific). Experiments in day-night conditions were performed in a separate day-night chamber, providing 12-hour light phase (~50 μE) followed by a 12-hour darkness phase.

Nitrogen starvation was induced by shifting the cells to nitrogen-free BG_{11} medium (BG_{11}^{0}) with an initial optical density at 750 nm (OD_{750}) of 0.5 and kept under constant light of 50 to 100 μE. For resuscitation assays, samples were taken after 7 and 14 days of nitrogen starvation, and the resuscitation was induced by shifting the cultures back to BG_{11}^{n}, as described previously (*19*, *46*). The osmotic stress was generated by addition of 50 to 600 mM sorbitol to BG_{11}^{n}, as indicated.

To generate long dark conditions, cultures were inoculated to a final OD_{750} of 0.4 and covered from light immediately using dark aluminum foil for 5 days and kept shaking at 28°C. To determine the recovery after prolonged darkness, samples were taken directly before shift to darkness (T_{zero}) and after 1, 2, 3, and 5 days of dark treatment and were recovered by shifting to 50 μE of white continuous light.

The agar drop assays were performed on BG_{11} agar plates containing 1.5% Bacto Agar (Thermo Fisher Scientific) in serial dilutions of OD_{750} ranging from 10^{0} to 10^{-4}, as described previously (*46*). To protect the freshly dropped cells from the photoinhibition, the agar plates were covered with white tissues for 24 hours after dropping, before they were exposed to the required conditions.

Oxygen measurements

To estimate oxygen levels in liquid cultures during 24 hours of diurnal rhythm, cultures were inoculated to a final OD_{750} of 0.4. Oxygen levels were measured in those cultures each 15 min using an Oxy-1 SMA (PreSens GmbH, Regensburg, Germany) device in combination with SP-PSt3-NAU-D5-YOP Oxygen Sensor Spots (PreSens GmbH). In contrast, the rate of C_i-dependent oxygen

evolution (oxygenic photosynthesis) as a function of increasing HCO_3^- concentration was determined using a Clark-type oxygen electrode (Hansatech), as previously described (*20*). All measurements were performed at least three times.

Estimation of intracellular glycogen concentration

Intracellular glycogen concentration was estimated as previously described (*7*) with modifications from (*19*). Cells were first exposed to two successive day-night cycles, followed by harvest of 40 ml of each culture within the mid of the third day phase.

Measurement of PSII activity by WATER-PAM chlorophyll fluorescence and the whole-cell spectra

On the basis of chlorophyll a fluorescence, PSII activity was determined using PAM fluorometry using a PAM control (Heinz Walz GmbH), as described previously (*20*, *47*), at a wavelength of 650 nm (measuring light). Shortly, the measurements were performed by diluting 20 µl of cells in H_2O to a final volume of 2 ml, followed by measuring every 30 s with the saturating pulse at either zero or 56 µE of actinic light. Samples were normalized to a fluorescence level of unexcited cells (F) that remained between 400 and 500 (*47*). The apparent PSII activity was determined with the saturation pulse method using the F_v/F_m ratio, where F_v defined as $F_m - F_0$.

Whole-cell spectra (320 to 750 nm; 5 nm s^{-1}) were recorded using a SPECORD 205 (Analytik Jena AG). Cultures were diluted 1:5 to a final volume of 1 ml.

Determination of intracellular c-di-AMP concentration

Samples for c-di-AMP measurement were taken throughout 24 hours. The first sample was taken immediately before the dark phase, the second sample 30 min after the onset of darkness, and subsequent samples every 2 hours afterward were harvested. The samples of the day phase were harvested in the same manner as for the night phase. Samples were taken from *Synechocystis sp.* PCC 6803 WT and Δ*dacA* cells. Illumination during light phase was at approximately 40 to 50 µE and during dark below 1 µE. Centrifugation steps were done at 20.800*g*, 4°C, and for 10 min. For sampling, 10 ml of cultures was filtered on a glass fiber prefilter (Merck Millipore Ltd., Cork, Ireland) with a pore size of 1.6 µm. Filters were then put in 2-ml reaction tubes, frozen in liquid nitrogen, and stored at −80°C until further processing. Samples were thawed in 700 µl of ice cold extraction solvent [acetonitrile/methanol/water (2/2/1, v/v/v)] and incubated in ice for 15 min. Afterward, they were heated for 10 min at 95°C, cooled on ice, and centrifuged, and the supernatant was transferred into a new tube. These steps, without the heating, were repeated twice with another 200 µl of extraction solvent. The combination of the supernatants from the three extractions was stored over night at −20°C. The next day, samples were centrifuged once more, supernatants were transferred to new tubes, and liquid were evaporated using a vacuum evaporator (Martin Christ Gefriertrocknungsanlagen GmbH, Osterode am Harz, Germany). The dried samples were resuspended in 200 µl of H_2O of which 40 µl was transferred into mass spectrometry vials filled with 40 µl of H_2O with $^{13}C_{20}{}^{15}N_{10}$-c-di-GMP and $^{13}C_{20}{}^{15}N_{10}$-c-di-AMP (200 ng/ml each). Further dilution, if necessary, was done with a solution of H_2O with $^{13}C_{20}{}^{15}N_{10}$-c-di-GMP and $^{13}C_{20}{}^{15}N_{10}$-c-di-AMP (100 ng/ml each). Calibrator preparation for mass spectrometry measurement was done with either 10 µl of cdiNMP-cGAMP calibrator cdZ0-13 or 10 µl of cdiNMP metabolites calibrator cdM0, 4-13. ddH_2O (40 µl) and ddH_2O (50 µl) with $^{13}C_{20}{}^{15}N_{10}$-c-di-GMP and $^{13}C_{20}{}^{15}N_{10}$-c-di-AMP (200 ng/ml each) were added and vortexed. Samples were heated at 95°C for 10 min, cooled on ice and frozen over night at −20°C. Samples were thawed, centrifuged, and transferred into MS vials with inserts.

Pull-down assays

Cell pellets of logarithmic growing *Synechocystis* WT or Δ*sbtB* cells were resuspended in 1 ml of detergent-free lysis buffer [50 mM tris-HCl, 50 mM NaCl, 50 mM KCl, 1 mM EDTA, 0.5 mM phenylmethylsulfonyl fluoride (pH 7.4)] and transferred into 1.5-ml microtubes containing 0.1 ml of glass beads (0.1 mm). Samples were lysed by using a FastPrep-24 Ribolyser (five cycles; 7.0 m s^{-1}; 30 s per cycle; 5-min break between each cycle; 4°C) and spun down at 10.000*g* and 4°C for 10 min. The supernatant was transferred into a fresh 1.5-ml reaction tube and kept on ice. The cyclic-di-AMP target fishing was performed as described (*48*), by passing the whole crude cell extract from WT *Synechocystis* sp. PCC 6803 cells growing under continuous illumination over 2′-AHC-c-diAMP agarose (catalog no. A183, BioLoG, Germany), while EtOH-NH agarose (catalog no. E010, BioLoG, Germany) was used as a negative control. The detection of SbtB in the c-di-AMP pull-down was confirmed by Western blot analysis using specific *Sc*SbtB-polyclonal antibodies as described previously (*20*).

For the strep-tag pull-down, 10 µM purified strep-tagged *Sc*SbtB was incubated with Δ*sbtB* crude cell extract (normalized to 3 mg of protein) of cells growing under continuous illumination, on 150 µl of MagStrep "type3" XT Beads (IBA GmbH) in the presence of either 2 mM cAMP (3′,5'-cAMP; Sigma-Aldrich, Germany) or 2 mM c-di-AMP (catalog no. C088, BioLoG, Germany) or without effector molecule in 1.5-ml reaction tubes at 28°C for 15 min. As a negative control, the same reaction was performed without purified *Sc*SbtB, to eliminate the proteins which could bind nonspecifically to the Strep beads. After discarding the supernatant, the column was washed three times with 1 ml of washing buffer [100 mM tris-HCl (pH 8.0), 150 mM NaCl, and 1 mM EDTA]. The elution was performed two times with 50 µl of BXT elution buffer (Biotin Elution Buffer, IBA GmbH), and both elution fractions were combined in a fresh 1.5-ml reaction tube. After measuring protein concentration by using a BCA Kit (Thermo Fisher Scientific), the whole sample was sent to liquid chromatography–mass spectrometry.

For the His_8-tag pull-down, 10 µM purified His-tagged SbtB was incubated with WT *Synechocystis* sp. PCC 6803 crude cell extract (normalized to 3 mg of protein) of cells growing under continuous illumination, on 150 µl of Ni-NTA MagBeads (Genaxxion) with either 0.1 mM c-di-AMP or without effector molecules in 1.5-ml reaction tubes at 28°C for 15 min. After discarding the supernatant, the column was washed five times with 1 ml of washing buffer [50 mM Na_2HPO_4 (pH 8.0), 300 mM NaCl, and 10 mM imidazole]. The elution was performed with 20 µl of elution buffer [50 mM Na_2HPO_4 (pH 8.0), 300 mM NaCl, and 250 mM imidazole].

For the SbtB, CoIP cell pellets of 300 ml logarithmic growing *Synechocystis* sp. PCC 6803 WT and Δ*sbtB* cells growing under continuous illumination (day condition) were resuspended in 1 ml of detergent-free lysis buffer [50 mM tris-HCl and 5 mM EDTA (pH 7.4)] and transferred into 1.5-ml microtubes containing 0.1 ml of glass beads (0.1 mm). Samples were lysed by using a FastPrep-24 Ribolyser (five cycles; 7.0 m s^{-1}; 30 s per cycle; 5-min break between

each cycle; 4°C) and spun down at 16.000*g* and 4°C for 5 min. The supernatant was transferred into a fresh 1.5-ml reaction tube and kept on ice. Aliquots of 150 µl of Protein G magnetic beads (Merck/Millipore PureProteome) were washed twice with 1 ml of lysis buffer and incubated with 60 µl of rabbit *Synechocystis* α-SbtB antiserum for 10 min at room temperature. After three additional washing steps, the beads were incubated under the previous coupling conditions with 3 mg of crude cell extract of either WT or Δ*sbtB*. After another three washing steps, elution was performed in two consecutive steps with each 60 µl of elution buffer (200 mM glycine buffer at pH 2.5). Both fractions were combined, shock-frozen in liquid nitrogen, and stored at −80°C until further analysis. As control for nonspecific binding, WT crude cell extract was incubated with rabbit *B. subtilis* α-TnrA antiserum coupled with Protein G magnetic beads.

For all of pull-down experiments, the eluted protein fractions were first subjected to the short SDS–polyacrylamide gel electrophoresis purification step, where the proteins were migrated into 12% gels for 1.5 cm and then stained with Coomassie blue, followed by in-gel digestion with Trypsin for the stained/isolated pieces of the gel-containing proteins. Trypsin-digested peptides were analyzed by liquid chromatography–tandem mass spectrometry on a Proxeon Easy-nLC coupled to Q Exactive HF, using linear gradient for 60 min. The spectra were searched against *Synechocystis* sp. PCC6803 database (UP000001425_1111708_complete_2019-02-13) and sequences for different versions of SbtB proteins (His-tagged or Strep-tagged). Label-free quantification was used to calculate intensities and iBAQ values that give semiquantitative quantifications of protein enrichment. The number of unique identified peptides/protein, sequence coverage, and score were considered to select proteins of interest.

GFP fluorescence quantification

The total amount of GFP fluorescence in the whole cells was determined as described previously in (*20*) for the Δ*sbtB* strain that expresses sbtB-sfGFP construct under the control of the native promoter of *sbtB* gene in successive day-night cycles. The emission of GFP fluorescence at 525 nm was determined for normalized cells of OD_{750} of 0.1, after excitation at 485 nm, using a Tecan multimode microplate reader (SparK 10M).

BACTH assay

Plasmid construction, cell cultivation, and experimental procedure of BACTH assay were performed as described previously (*49*) only on X-Gal plates supplemented with X-Gal (40 µg/ml), kanamycin (50 µg/ml), ampicillin (100 µg/ml), and IPTG (1 mM). We tested only the N-terminal fusion of T25 subunit of Cya to SbtB, while the T18 subunit of Cya was fused either N- or C-terminally to the glycogen-related enzymes GlgA1, GlgA2, GlgP1, GlgP2, GlgB, and GlgC. Primers used to generate T25-SbtB fusion protein are listed in (table S1). The T25-SbtB fusion with an empty pUT18 vector was used as negative control, while the leucine zipper interaction was used as positive control. The *E. coli* BTH101 (Euromedex) was used for BACTH assays. The BACTH assays were performed at least three-times with three independent *E. coli* colonies to confirm the reproducibility and the specificity of the SbtB-GlgB interaction.

Microscale thermophoresis

MST experiments were carried out as previously described (*20*) using a Monolith NT.115 (NanoTemper Technologies GmbH) with uncoated Monolith NT.115 Capillaries (NanoTemper Technologies GmbH). Primary amines (lysine residues) of His-tagged GlgB were fluorescent labeled using the Monolith Protein Labeling Kit RED-NHS (NanoTemper Technologies GmbH). Titration series of StrepII-tagged *Sc*SbtB in the range of 1.3 nM to 42.5 µM were incubated with 10 nM fluorescent labeled His-tagged GlgB in 50 mM phosphate buffer (pH 8.0). All runs were performed in triplicate with 40% MST power and 60% light-emitting diode power. Single-site fitting was done using the NanoTemper data analysis software.

Isothermal titration calorimetry

ITC experiments were performed as previously described (*20*, *50*) using a VP-ITC microcalorimeter (MicroCal) in 50 mM sodium-potassium phosphate buffer (pH 8.0) supplemented with 0.5 mM EDTA, at 20°C. For determination of binding isotherms of small effector molecules binding to *Sc*SbtB, the protein (33.3 µM trimer concentration) was titrated against 0.5 or 1.0 mM c-di-AMP sodium salt (catalog no. C088, BioLoG, Germany).

SUPPLEMENTARY MATERIALS

Supplementary material for this article is available at https://science.org/doi/10.1126/sciadv.abk0568

View/request a protocol for this paper from *Bio-protocol*.

REFERENCES AND NOTES

1. D. G. Welkie, B. E. Rubin, S. Diamond, R. D. Hood, D. F. Savage, S. S. Golden, A hard day's night: Cyanobacteria in diel cycles. *Trends Microbiol.* **27**, 231–242 (2019).
2. Z. Eelderink-Chen, J. Bosman, F. Sartor, A. N. Dodd, Á. T. Kovács, M. Merrow, A circadian clock in a nonphotosynthetic prokaryote. *Sci. Adv.* **7**, eabe2086 (2021).
3. D. G. Welkie, B. E. Rubin, Y. G. Chang, S. Diamond, S. A. Rifkin, A. LiWanga, S. S. Golden, Genome-wide fitness assessment during diurnal growth reveals an expanded role of the cyanobacterial circadian clock protein KaiA. *Proc. Natl. Acad. Sci. U.S.A.* **115**, E7174–E7183 (2018).
4. N. Wan, D. M. DeLorenzo, L. He, L. You, C. M. Immethun, G. Wang, E. E. K. Baidoo, W. Hollinshead, J. D. Keasling, T. S. Moon, Y. J. Tang, Cyanobacterial carbon metabolism: Fluxome plasticity and oxygen dependence. *Biotechnol. Bioeng.* **114**, 1593–1602 (2017).
5. A. Makowka, L. Nichelmann, D. Schulze, K. Spengler, C. Wittmann, K. Forchhammer, K. Gutekunst, Glycolytic Shunts Replenish the Calvin–Benson–Bassham Cycle as Anaplerotic Reactions in Cyanobacteria. *Mol. Plant* **13**, 471–482 (2020).
6. C. Köbler, S. J. Schultz, D. Kopp, K. Voigt, A. Wilde, The role of the *Synechocystis* sp. PCC 6803 homolog of the circadian clock output regulator RpaA in day–night transitions. *Mol. Microbiol.* **110**, 847–861 (2018).
7. M. Gründel, R. Scheunemann, W. Lockau, Y. Zilliges, Impaired glycogen synthesis causes metabolic overflow reactions and affects stress responses in the cyanobacterium *Synechocystis* sp. PCC 6803. *Microbiology* **158**, 3032–3043 (2012).
8. S. Diamond, D. Jun, B. E. Rubin, S. S. Golden, The circadian oscillator in *Synechococcus elongatus* controls metabolite partitioning during diurnal growth. *Proc. Natl. Acad. Sci. U.S.A.* **112**, E1916–E1925 (2015).
9. R. D. Hood, S. A. Higgins, A. Flamholz, R. J. Nichols, D. F. Savage, The stringent response regulates adaptation to darkness in the cyanobacterium *Synechococcus elongatus*. *Proc. Natl. Acad. Sci. U.S.A.* **113**, E4867–E4876 (2016).
10. A. M. Puszynska, E. K. O'Shea, ppGpp controls global gene expression in light and in darkness in *S. elongatus*. *Cell Rep.* **21**, 3155–3165 (2017).
11. B. E. Rubin, T. N. Huynh, D. G. Welkie, S. Diamond, R. Simkovsky, E. C. Pierce, A. Taton, L. C. Lowe, J. J. Lee, S. A. Rifkin, J. J. Woodward, S. S. Golden, High-throughput interaction screens illuminate the role of c-di-AMP in cyanobacterial nighttime survival. *PLOS Genet.* **14**, e1007301 (2018).
12. J. He, W. Yin, M. Y. Galperin, S. H. Chou, Cyclic di-AMP, a second messenger of primary importance: Tertiary structures and binding mechanisms. *Nucleic Acids Res.* **48**, 2807–2829 (2020).
13. W. Yin, X. Cai, H. Ma, L. Zhu, Y. Zhang, S. H. Chou, M. Y. Galperin, J. He, A decade of research on the second messenger c-di-AMP. *FEMS Microbiol. Rev.* **44**, 701–724 (2020).
14. J. Stülke, L. Krüger, Cyclic di-AMP Signaling in Bacteria. *Annu. Rev. Microbiol.* **74**, 159–179 (2020).
15. J. Gundlach, A. Dickmanns, K. Schröder-Tittmann, P. Neumann, J. Kaesler, J. Kampf, C. Herzberg, E. Hamemr, F. Schwede, V. Kaever, K. Tittmann, J. Stülke, R. Ficner,

Identification, characterization, and structure analysis of the cyclic di-AMP-binding PII-like signal transduction protein DarA. *J. Biol. Chem.* **290**, 3069–3080 (2015).
16. I. Campeotto, Y. Zhang, M. G. Mladenov, P. S. Freemont, A. Gründling, Complex structure and biochemical characterization of the staphylococcus aureus Cyclic Diadenylate Monophosphate (c-di-AMP)-binding Protein PstA, the Founding Member of a New Signal Transduction Protein Family. *J. Biol. Chem.* **290**, 2888–2901 (2015).
17. M. Agostoni, A. R. Logan-Jackson, E. R. Heinz, G. B. Severin, E. L. Bruger, C. M. Waters, B. L. Montgomery, Homeostasis of Second Messenger Cyclic-di-AMP Is Critical for Cyanobacterial Fitness and Acclimation to Abiotic Stress. *Front. Microbiol.* **9**, 1121 (2018).
18. J. W. Nelson, N. Sudarsan, K. Furukawa, Z. Weinberg, J. X. Wang, R. R. Breaker, Riboswitches in eubacteria sense the second messenger c-di-AMP. *Nat. Chem. Biol.* **9**, 834–839 (2013).
19. A. Klotz, J. Georg, L. Bučinská, S. Watanabe, V. Reimann, W. Januszewski, R. Sobotka, D. Jendrossek, W. R. Hess, K. Forchhammer, Awakening of a Dormant Cyanobacterium from Nitrogen Chlorosis Reveals a Genetically Determined Program. *Curr. Biol.* **26**, 2862–2872 (2016).
20. K. A. Selim, F. Haase, M. D. Hartmann, M. Hagemann, K. Forchhammer, PII-like signaling protein SbtB links cAMP sensing with cyanobacterial inorganic carbon response. *Proc. Natl. Acad. Sci. U.S.A.* **115**, 4861–4869 (2018).
21. N. Oren, S. Timm, M. Frank, O. Mantovani, O. Murik, M. Hagemann, Red/far-red light signals regulate the activity of the carbon-concentrating mechanism in cyanobacteria. *Sci. Adv.* **7**, eabg0435 (2021).
22. J. Du, B. Förster, L. Rourke, S. M. Howitt, G. D. Price, Characterisation of Cyanobacterial Bicarbonate Transporters in *E. coli* Shows that SbtA Homologs Are Functional in This Heterologous Expression System. *PLOS ONE* **9**, 12 (2014).
23. S. Fang, X. Huang, X. Zhang, M. Zhang, Y. Hao, H. Guo, L. N. Liu, F. Yu, P. Zhang, Molecular mechanism underlying transport and allosteric inhibition of bicarbonate transporter SbtA. *Proc. Natl. Acad. Sci. U.S.A.* **118**, e2101632118 (2021).
24. T. Lapina, K. A. Selim, K. Forchhammer, E. Ermilova, The PII signaling protein from red algae represents an evolutionary link between cyanobacterial and Chloroplastida PII proteins. *Sci. Rep.* **8**, 790 (2018).
25. K. A. Selim, E. Ermilova, K. Forchhammer, From cyanobacteria to Archaeplastida: New evolutionary insights into PII signalling in the plant kingdom. *New Phytol.* **227**, 722–731 (2020).
26. Y. Chen, M. J. Cann, T. N. Litvin, V. Iourgenko, M. L. Sinclair, L. R. Levin, J. Buck, Soluble adenylyl cyclase as an evolutionarily conserved bicarbonate sensor. *Science* **289**, 625–628 (2000).
27. J. A. Kaczmarski, N. S. Hong, B. Mukherjee, L. T. Wey, L. Rourke, B. Förster, T. S. Peat, G. D. Price, C. J. Jackson, Structural Basis for the Allosteric Regulation of the SbtA Bicarbonate Transporter by the PII-like Protein, SbtB, from *Cyanobium* sp. PCC7001. *Biochemistry* **58**, 5030–5039 (2019).
28. J. Gundlach, L. Krüger, C. Herzberg, A. Turdiev, A. Poehlein, I. Tascón, M. Weiss, D. Hertel, R. Daniel, I. Hänelt, V. T. Lee, J. Stülke, Sustained sensing in potassium homeostasis: Cyclic di-AMP controls potassium uptake by KimA at the levels of expression and activity. *J. Biol. Chem.* **294**, 9605–9614 (2019).
29. K. Forchhammer, K. A. Selim, Carbon/nitrogen homeostasis control in cyanobacteria. *FEMS Microbiol. Rev.* **44**, 33–53 (2020).
30. R. Saha, D. Liu, A. Hoynes-O'Connor, M. Liberton, J. Yu, M. Bhattacharyya-Pakrasi, A. Balassy, F. Zhang, T. Seok Moon, C. D. Maranas, H. B. Pakrasi, Diurnal regulation of cellular processes in the cyanobacterium *Synechocystis* sp. Strain PCC 6803: Insights from transcriptomic, fluxomic, and physiological analyses. *MBio* **7**, e00464-16 (2016).
31. E. Suzuki, H. Ohkawa, K. Moriya, T. Matsubara, Y. Nagaike, I. Iwasaki, S. Fujiwara, M. Tsuzuki, Y. Nakamura, Carbohydrate metabolism in mutants of the cyanobacterium *Synechococcus elongatus* PCC 7942 defective in glycogen synthesis. *Appl. Environ. Microbiol.* **76**, 3153–3159 (2010).
32. S. Doello, A. Klotz, A. Makowka, K. Gutekunst, K. Forchhammer, A specific glycogen mobilization strategy enables rapid awakening of dormant cyanobacteria from chlorosis. *Plant Physiol.* **177**, 594–603 (2018).
33. A. Wiegard, C. Köbler, K. Oyama, A. K. Dörrich, C. Azai, K. Terauchi, A. Wilde, I. M. Axmann, *Synechocystis* KaiC3 displays temperature- and KaiB-dependent ATPase activity and is important for growth in darkness. *J. Bacteriol.* **202**, e00478-19 (2020).
34. H. Iijima, T. Shirai, M. Okamoto, A. Kondo, M. Y. Hirai, T. Osanai, Changes in primary metabolism under light and dark conditions in response to overproduction of a response regulator RpaA in the unicellular cyanobacterium *Synechocystis* sp. PCC 6803. *Front. Microbiol.* **6**, 888 (2015).
35. S. Berry, B. Esper, I. Karandashova, M. Teuber, I. Elanskaya, M. Rögner, M. Hagemann, Potassium uptake in the unicellular cyanobacterium *Synechocystis* sp. strain PCC 6803 mainly depends on a Ktr-like system encoded by slr1509 (ntpJ). *FEBS Lett.* **548**, 53–58 (2003).
36. N. Matsuda, H. Kobayashi, H. Katoh, T. Ogawa, L. Futatsugi, T. Nakamura, E. P. Bakker, N. Uozumi, Na^+-dependent K^+ Uptake Ktr System from the Cyanobacterium *Synechocystis* sp. PCC 6803 and Its Role in the Early Phases of Cell Adaptation to Hyperosmotic Shock. *J. Biol. Chem.* **279**, 54952–54962 (2004).
37. A. C. Pohland, D. Schneider, D, Mg^{2+} homeostasis and transport in cyanobacteria - at the crossroads of bacterial and chloroplast Mg^{2+} import. *Biol. Chem.* **400**, 1289–1301 (2019).
38. V. Shyp, B. N. Dubey, R. Böhm, J. Hartl, J. Nesper, J. A. Vorholt, S. Hiller, T. Schirmer, U. Jenal, Reciprocal growth control by competitive binding of nucleotide second messengers to a metabolic switch in *Caulobacter crescentus*. *Nat. Microbiol.* **6**, 59–72 (2021).
39. K. Forchhammer, J. Lüddecke, Sensory properties of the PII signalling protein family. *FEBS J.* **283**, 425–437 (2016).
40. M. Eisenhut, E. A. von Wobeser, L. Jonas, H. Schubert, B. W. Ibelings, H. Bauwe, H. C. Matthijs, M. Hagemann, Long-term response toward inorganic carbon limitation in wild type and glycolate turnover mutants of the cyanobacterium *Synechocystis* sp. strain PCC 6803. *Plant Physiol.* **144**, 1946–1959 (2007).
41. J. K. Gupta, P. Rai, K. K. Jain, S. Srivastava, Overexpression of bicarbonate transporters in the marine cyanobacterium *Synechococcus* sp. PCC 7002 increases growth rate and glycogen accumulation. *Biotechnol. Biofuels* **13**, 17 (2020).
42. K. A. Selim, L. Tremiño, C. Marco-Marín, V. Alva, J. Espinosa, A. Contreras, M. D. Hartmann, K. Forchhammer, V. Rubio, Functional and structural characterization of PII-like protein CutA does not support involvement in heavy metal tolerance and hints at a small-molecule carrying/signaling role. *FEBS J.* **288**, 1142–1162 (2021).
43. W. Kabsch, XDS. *Acta Crystallogr. D Biol. Crystallogr.* **66**, 125–132 (2010).
44. G. N. Murshudov, P. Skubák, A. A. Lebedev, N. S. Pannu, R. A. Steiner, R. A. Nicholls, M. D. Winn, F. Long, A. A. Vagin, REFMAC5 for the refinement of macromolecular crystal structures. *Acta Crystallogr. D Biol. Crystallogr.* **67**, 355–367 (2011).
45. D. Trautmann, B. Voss, A. Wilde, S. Al-Babili, W. R. Hess, Microevolution in cyanobacteria: Re-sequencing a motile substrain of Synechocystis sp. PCC 6803. *DNA Res.* **19**, 435–448 (2012).
46. K. A. Selim, M. Haffner, Heavy Metal Stress Alters the Response of the Unicellular Cyanobacterium *Synechococcus elongatus* PCC 7942 to Nitrogen Starvation. *Life* **10**, 275 (2020).
47. A. M. Acuna, J. J. Snellenburg, M. Gwizdala, D. Kirilovsky, R. Van Grondelle, I. H. M. Van Stokkum, Resolving the contribution of the uncoupled phycobilisomes to cyanobacterial pulse-amplitude modulated (PAM) fluorometry signals. *Photosynth. Res.* **127**, 91–102 (2016).
48. J. Kampf, J. Gundlach, C. Herzberg, K. Treffon, J. Stülke, Identification of c-di-AMP-Binding Proteins Using Magnetic Beads, in *c-di-GMP Signaling: Methods and Protocols. Methods in Molecular Biology* (Springer, Science+Business Media LLC, Berlin, 2017), pp. 347–359.
49. B. Watzer, P. Spät, N. Neumann, M. Koch, R. Sobotka, B. Macek, O. Hennrich, K. Forchhammer, The signal transduction protein P_{II} controls ammonium, nitrate and urea uptake in cyanobacteria. *Front. Microbiol.* **10**, 1428 (2019).
50. K. A. Selim, M. Haffner, B. Watzer, K. Forchhammer, Tuning the *in vitro* sensing and signaling properties of cyanobacterial PII protein by mutation of key residues. *Sci. Rep.* **9**, 18985 (2019).

Acknowledgments: We are grateful to A. Klotz and H. Grenzendorf (IMIT, Tübingen University) for the excellent assistance, the staff of beamline X10SA/SLS, the Proteome Center (Tübingen University), W. R. Hess (Freiburg University) for the microarray data, and L. Lo-Presti for critical scientific and linguistic editing of the manuscript. Furthermore, we would like to acknowledge the infrastructural support by the Cluster of Excellence "Controlling Microbes to Fight Infections" (EXC 2124–390838134) of the DFG. K.A.S. would like to dedicate this research to the memory of A. Selim, a distinguished father and medical doctor, for the continued support. **Funding:** This work was supported by the German research foundation (DFG) within the priority program SPP1879 to (K.F., M.Hag., M.Haf., and O.M.) and by institutional funds of the Max Planck Society. DFG-Cluster of Excellence (EXC 2124) "Controlling Microbes to Fight Infections" to (K.A.S.). **Author contributions:** K.A.S. and K.F. conceived, initiated, and supervised the whole project. K.A.S. designed the experiments. M.Haf. and K.A.S. performed most of the physiological and biochemical experiments, except for c-di-AMP quantification by M.B. with help of R.S., photosynthetic HCO_3^--dependent oxygen evolution by O.M. under supervision of M.Hag., and BACTH by N.N. L.K. and J.S. helped M.Haf. for performing c-di-AMP pull-down. R.A. performed crystallographic sample preparation and diffraction data collection, K.A.S. solved the crystal structure, and M.D.H. supervised the structural analysis. K.A.S. evaluated and interpreted the results, prepared the figures, and wrote the manuscript. K.A.S., M.D.H., M.Hag., and K.F. commented and edited on the manuscript. All authors approved the final version of the manuscript. **Competing interests:** The authors declare that they have no competing interests. **Data and materials availability:** Crystallography, atomic coordinates, and structure factors have been deposited in the Protein Data Bank, www.wwpdb.org (PDB ID code: 7OBJ).

Submitted 18 June 2021
Accepted 18 October 2021
Published 8 December 2021
10.1126/sciadv.abk0568